FLOATING PISTON EXPANDER DEVELOPMENT FOR A SMALL-SCALE COLLINS TYPE 10 K CRYOCOOLER FOR SPACE APPLICATIONS

C.L. Hannon[1], J. Gerstmann[1], B.J. Krass[1],
M.J. Traum[2], J.G. Brisson[2] and J.L. Smith Jr[2].

[1]Advanced Mechanical Technology, Inc.
Watertown, MA, 02472, USA

[2]Cryogenic Engineering Laboratory
MIT, Cambridge, MA, USA

ABSTRACT

Future spacecraft cooling and sensing systems will require advanced multi-stage cryocoolers capable of providing continuous cooling at multiple temperature levels ranging from 10 K to 95 K. Stirling and pulse-tube cryocoolers have achieved compactness and reliability by adopting mechanically simple cold head configurations at the expense of thermodynamic efficiency. Large-scale terrestrial cryogenic refrigerators achieve much higher efficiencies by employing complex designs, but their high efficiency is not retained at the small scale required for spacecraft cryogenic cooling. AMTI, in collaboration with MIT, is developing a multi-stage 10 K cryocooler that applies modern microelectronic sophistication to achieve high efficiency in a reliable, compact design. The cryocooler is based upon a novel modification of the Collins cycle, a cycle commonly used in many high-efficiency terrestrial cryogenic machines. Innovations of the design include *floating piston expanders* and electro-magnetic *smart valves*, which eliminate the need for mechanical linkages and reduce the input power, size, and weight of the cryocooler in an affordable modular design. This paper will present the design of the first generation prototype, the results of development testing, and the direction of future development efforts.

CP710, *Advances in Cryogenic Engineering: Transactions of the Cryogenic Engineering Conference - CEC, Vol. 49,* edited by J. Waynert et al.

INTRODUCTION

Many current cryocoolers, most notably Stirling and pulse-tube types, have achieved compactness and reliability by adopting mechanically simple cold head configurations at the expense of thermodynamic efficiency. Large multi-stage terrestrial cryogenic refrigerators are able to achieve higher thermodynamic efficiencies, but do so by employing mechanically complex designs that are not feasible at a small scale. The ideal 10 K spacecraft cryocooler would have an efficiency comparable to that of large terrestrial machines, i.e., a power requirement less than 1 kW per watt of cooling at 10 K, with the compactness and reliability of a pulse-tube or Stirling cryocooler. An efficient multi-stage 10 K cryocooler with many of the above attributes is currently under development by AMTI in collaboration with the Cryogenic Engineering Laboratory at MIT. This design achieves compactness and reliability by using modern microelectronics to enable a complex, but efficient, cold head design. The cryocooler is based upon a novel modification of the Collins cycle that is used in many high-efficiency terrestrial cryogenic machines. The technology concepts enabling this innovative design are presented in [1]. A system schematic is illustrated in FIGURE 1.

A comparison of the thermodynamic performance of refrigeration at 4 K clearly shows the potential for successful cryocooler design using the new paradigm. The large-scale, high-efficiency machines based on the conventional Brayton and Collins cycles routinely operate with input powers of about 740 W per watt of refrigeration, which is only 10 times the ideal Carnot power at 4 K. Small commercial sub-10 K Gifford-McMahon cryocoolers capable of about 1W of cooling at 4 K have been available for several years (Daikin, Sumitomo, Leybold). These devices typically require about 5 kW - 7.5 kW per watt of cooling at 4 K, which is about 70 to 100 times the Carnot requirement [2]. The modified Collins cycle under development is particularly well suited for cryocoolers operating from below 4 K up to about 30 K, above which temperature the thermodynamic losses of the mechanically simpler cryocoolers become less dominant.

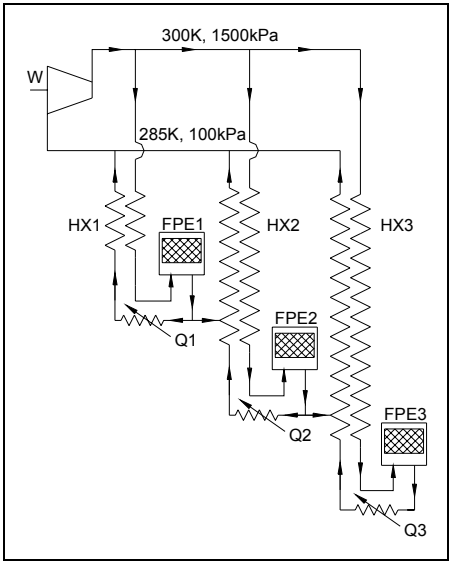

FIGURE 2. Modified Collins Cycle

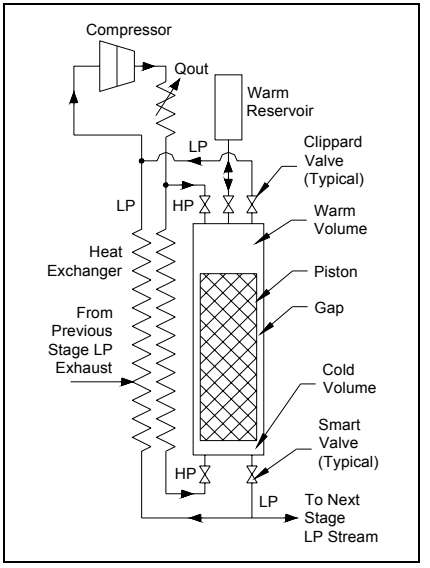

FIGURE 1. Floating Piston Expander

PROTOTYPE FLOATING PISTON EXPANDER

The *floating piston expander* (FPE), first studied by Jones [3] and further developed by Smith [4], illustrated conceptually in FIGURE 2, is a key element in the cryocooler concept. By employing a floating piston, the expander provides a highly effective expansion at a high-pressure ratio without the size, weight, and geometric constraints of a mechanical crosshead to stroke the piston and operate the cold valves via pull rods. The expander consists of a piston (or displacer) that floats with the gas in a closed cylinder. At the cold-end of the cylinder, high-pressure gas is admitted through a smart electromagnetic inlet valve, and low-pressure gas exits through a smart electromagnetic exhaust valve. A microprocessor controls the opening and closing of the valves to achieve efficient expansion of the gas, and to minimize losses in the valves. The piston floating in the cylinder moves to keep the pressure in the warm-end displacement volume nearly the same as the pressure in the cold-end volume. The warm end has multiple electromagnetic valves that connect to reference-pressure reservoirs. The warm end valves are flow-control throttling valves that control the velocity of the floating piston by controlling the rate of gas flow into and out of the warm cylinder volume. With this configuration, the helium pressure on the warm end of the piston is always essentially the same as the pressure on the cold end. The piston floats quasi-statically on the gas in the cylinder with low velocities set by the throttling of the gas in and out of the warm cylinder volume. The cold valves always open when there is essentially no pressure difference across the valve. This reduces the actuating force required of the cold valve actuators.

FIGURE 2 illustrates the general configuration of the first prototype FPE built for this project. Four valves at the warm-end control gas flow in and out of the warm-end volume. The high pressure gas source acted as the highest reference-pressure reservoir, and the atmosphere acted as the lowest reference-pressure reservoir. A single intermediate-pressure reservoir was provided that was connected to the warm-end volume by two valves. (For clarity in FIGURE 2, only one valve is shown connecting to the reservoir.)

The FPE prototype was supplied with prototype electro-magnetic *smart valves* at the cold end. The design for these valves is based on U.S. Patent 5,211,372, but the specific configuration of these valves has evolved significantly. An improved valve configuration has evolved from the need to fully utilize the available diameter of the expander for active magnetic components, coils and cores. As shown in FIGURE 3, the valve arrangement is a concentric design, with the exhaust valve located concentricly outside of the inlet valve. For both the inlet and exhaust valves, action is by the motion of a valve disk relative to a valve plate, which is also the cylinder head of the expander. When against the plate, the valve disk is held against the valve seats by the gas pressure difference across the valve ports and by permanent magnets acting as a valve spring. The valve is opened by a magnetic field that pulls the valve disk away from the plate. The valve port area of each valve consists of three small-diameter holes through the plate equally spaced on a circle. As in compressor valves, multiple ports with small dimensions provide a small valve lift for the required flow area. The small lift allows an optimum magnetic design for a quick opening and closing valve with minimum impact stress.

A toroidal yoke of ferromagnetic stainless steel surrounds a ring coil of copper wire. The valve disk of ferromagnetic stainless steel is separated from the flat face of the yoke by a small air gap that decreases as the valve disk moves to open the valve. When current flows in the coil, magnetic field flows through the yoke, across the air gap, through the valve disk and back to the yoke creating closed flux lines around the coil. The magnetic field crossing the air gap causes an attractive force between the valve yoke and the valve disk. This attractive force is sufficient to lift the valve disk off of the non-magnetic cylinder head plate against the gas pressure difference across the valve. A large flux path

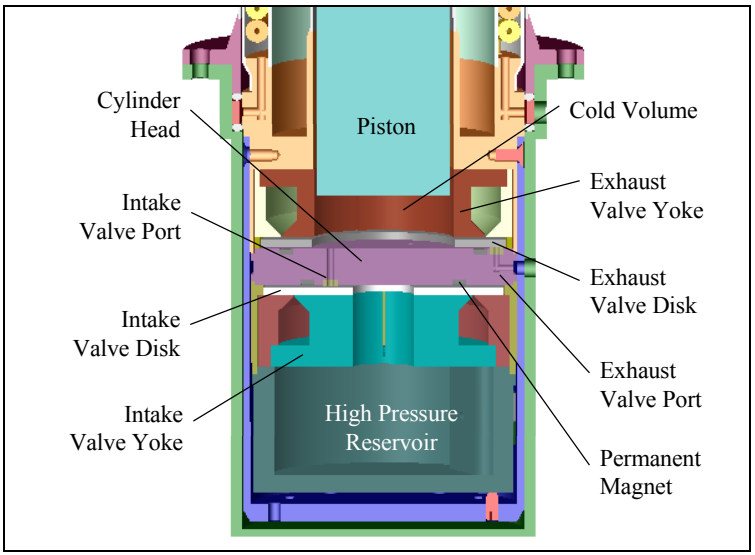

FIGURE 3. Electromagnetic *Smart Valve*

area and a small air gap thickness give a large force for a given number of ampere-turns in the coil. When the current is turned off the attractive force between the yoke and the disk is near zero (there is some residual magnetic flux in the yoke). The disk is pulled back to the cylinder head plate by permanent magnets mounted in the plate and by the pressure difference generated as the gas flow is interrupted.

The circuits that supply current to the valve actuator coils are designed to minimize the resistive (I^2R) heating in the cold valve coils. A high current pulse is supplied for a few milliseconds to crack the valve open. As the valve opens, the pressure differential across the valve decreases rapidly as does the force from the permanent magnets. This allows a much lower current level to complete the valve opening and hold the valve open for the 70-100 milliseconds required to complete an intake or exhaust event. (The small air gap in the magnetic flux path when the valve is open requires only a low current level to produce a sufficiently high magnetic force between the valve disk and the yoke so that the valve is held open.) Since resistive heating in the coil is proportional to the square of the current level, this approach reduces the resistive heating load integrated over a complete intake or exhaust event to less than 1 mW. The resistive losses in the ring coil are much lower when the coil is at 10 K than when it is at room temperature because the resistance of copper is at least 1/30 of its room temperature resistance and can easily be as low as 1/80 for extra-high-purity copper.

A typical current-voltage response is shown in FIGURE 4. To initiate actuation of the intake valve, the voltage is driven to its extreme negative potential which results in a rapid current rise to about 140 mAmps which was the pre-set peak current pulse level. After about 6 msec, the voltage is driven to its positive extreme to rapidly reduce the current from the peak level to its pre-set holding level of 20 mAmps. Only a nominal voltage is required to supply the holding current. To close the valve, the voltage is again driven positive to pull the current down to zero, at which point the voltage rapidly decays to zero. Transients can be seen in the voltage trace at the valve opening that are related to the dynamics of the valve disk and its effect on the magnetic field and coil inductance.

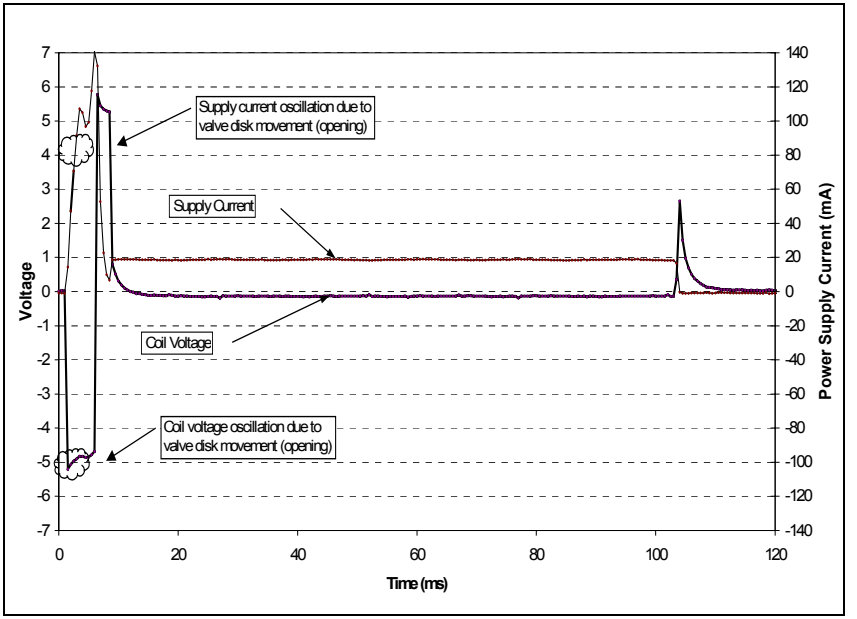

FIGURE 4. *Smart Valve* Shaped Voltage-Current Pulse

FPE PERFORMANCE

The ideal steady-state expansion cycle for the FPE is shown in FIGURE 5 as a pressure vs. volume (PV) diagram. It consists of a constant high-pressure intake stroke (state 1 to state 2), an expansion to intermediate-pressure (state 2 to state 3), further expansion to low-pressure (state 3 to state 4), a constant low-pressure exhaust stroke (state 4 to state 5), recompression to intermediate-pressure (state 5 to state 6), and final recompression to high-pressure (state 6 to state 1).

The expander cycle starts with the piston in the position where the cold volume, V_c is a minimum and the pressure is at the compressor discharge pressure, P_h. The piston is floating so that the pressure in the warm volume, V_w, is the same as in the cold volume, V_c. The two cold valves, V_{in} and V_{ex}, and the warm valves, V_1, V_{2a}, V_{2b}, and V_3 are all closed. Since the cylinder is of constant cross section, the cold volume is proportional to piston displacement. Piston displacement was tracked by Hall effect sensors located outside of the cylinder that measured the radial magnetic field emitted by a stack of permanent magnets embedded in the piston. The field strength varied linearly with displacement for displacements within the North and South poles of the magnet stack. As such, X_c, is the height of the cold volume, V_c. Timing of the intake and exhaust processes was based on a comparisons to the predetermined intake cutoff displacement, X_{co}, and recompression displacement, X_{rc}.

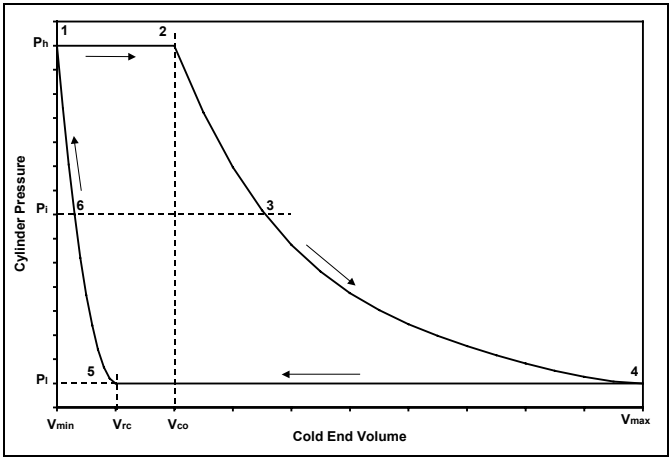

FIGURE 5. Ideal Cycle P-V Diagram

A LabView based data acquisition and control algorithm was developed to monitor cylinder pressure and piston displacement, and to actuate the warm and cold-end valves according to the logic in TABLE 1. During early testing of the FPE prototype it also became clear that Valve 3 did not reduce the cylinder pressure all the way to P_l by the time the piston had reached the end of the expansion stroke. As a result, when Valve 3 was closed, differential pressure existed across the piston when the exhaust valve was opened to begin the exhaust stroke. This resulted in significant net force on the piston causing a downward acceleration. The value of X_{rc} needed to be set very high to avoid piston impact at the cold end. The solution to this problem was the addition of a release process after the second expansion. When the piston reached its maximum displacement, Valve 3 remained open when the exhaust valve was opened. This held the piston at the warm end while the cylinder pressure bled down to P_l. At that point, Valve 3 was closed and Valve 2a was opened to begin the exhaust process.

FIGURE 6 presents cylinder pressure and piston position data. Four data sets recorded at different times but with the same operating parameters are plotted as well as a fifth data set recorded after the X_{co} value had been reduced. The first four data sets lie right

TABLE 1. FPE Valve Logic

Process	1-2 Intake	2-3 First Expansion	3-4 Second Expansion	Release	4-5 Exhaust	5-6 First Recompression	6-1 Second Recompression
Criteria	$X_c < X_{co}$	$P_{cyl} > P_{int}$	$P_{cyl} > P_{low}$	$X_c \sim X_{max}$	$X_c > X_{rc}$	$P_{cyl} < P_{int}$	$P_{cyl} < P_{int}$
V_{in}	**Open**	Closed	Closed	Closed	Closed	Closed	Closed
V_{ex}	Closed	Closed	Closed	**Open**	**Open**	Closed	Closed
V_1 (P_h)	Closed	Closed	Closed	Closed	Closed	Closed	**Open**
V_{2a} (P_i)	**Open**	**Open**	Closed	Closed	**Open**	**Open**	Closed
V_{2b} (P_i)	Closed	**Open**	Closed	Closed	Closed	**Open**	Closed
V_3 (P_l)	Closed	Closed	**Open**	**Open**	Closed	Closed	Closed

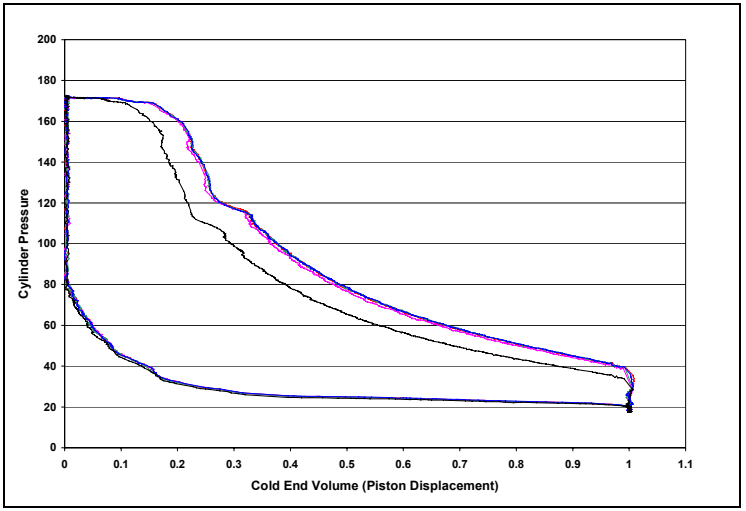

FIGURE 6. Multi-Cycle P-V Diagram

on top of each other demonstrating the repeatability of the expansion cycle. The fifth cycle is notable because the expansion curve has the same characteristic shape as the first four data sets, but it is translated to the left because of the shorter cut off.

With warm-end connections to the high-pressure source and to atmosphere, a significant amount of high pressure gas bypassed the cold-end expansion volume. This configuration was chosen so that at the start of both the intake and exhaust events, the pressure difference across the piston would be nearly zero. This would prevent rapid and uncontrollable piston acceleration. Experience with the first FPE configuration demonstrated that piston dynamics were controllable even with small pressure differences across the piston. An alternative warm-end configuration was built that eliminated the connections to the high-pressure source and to atmosphere. Instead, four reservoirs were installed so that the warm-end was closed.

In this configuration, pressure in each of the four reservoirs was pre-set. The highest pressure was slightly less than the system high pressure level and the lowest pressure was set slightly higher than the system low pressure level (atmospheric pressure). The other two reservoirs were set to a high-intermediate pressure and low-intermediate pressure, respectively. In operation, the four reservoir pressures self-adjusted to steady state levels based on the valve timing criteria. A resulting cycle P-V diagram is shown in FIGURE 7. It has the same general shape as FIGURE 6, but it should be noted that the intake process begins at a cylinder pressure slightly less than high-pressure, and the exhaust process begins at a pressure slightly higher than low-pressure. These conditions resulted in larger pressure differences across the piston, but the resulting piston velocities were controllable. The great benefit of this configuration was elimination of a net mass flow through the warm-end volume.

PROJECT STATUS

The project has demonstrated *floating piston expanders* equipped with electromagnetically actuated cryogenic *smart valves*. A LabView based computer has been developed to enable continuous cyclic operation with the ability to alter cycle parameters

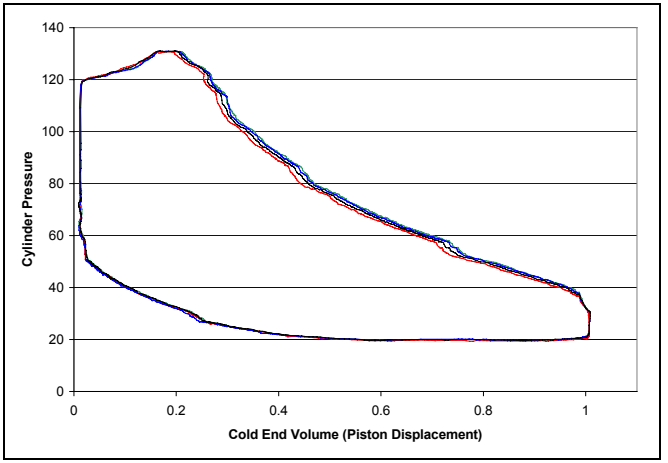

FIGURE 7. Four-Reservoir Multi-Cycle P-V Diagram

on-the-fly. Having demonstrated the key technologies required to enable the modified Collins cryocooler cycle, the 10 K stage of the three-stage cryocooler has been designed and is currently nearing final assembly. This single-stage cryocooler prototype will incorporate a recuperative heat exchanger with the FPE to demonstrate cooling at 10 K. Testing is expected to begin by late Fall 2003.

ACKNOWLEDGEMENTS

This work has been supported by an SBIR Grants from the Missile Defense Agency, Contract No. DASG60-01-C-0051 administered by the U.S. Army Space and Missile Defense Agency, and Contract No. F29601-02-C-0155 administered by the U.S. Air Force Research Laboratory.

REFERENCES

1. Hannon, C.L., Gerstmann, J., Traum, M., Brisson, J.G., Smith Jr, J.L., "Development of a Medium-Scale Collins-Type 10 K Cryocooler," in *Cryocoolers* 12, Ross Jr, R.G., ed., Kluwer Academic/Plenum Publishers, New York, 2003, pp. 587-594.

2. L. D'Addario, "Review of Gifford-McMahon Refrigerators for 4 K," Millimeter Array (MMA) Project MMA Memo #185, http://www.alma.nrao.edu/memos/html-memos/alma185/mma185.txt, September 25, 1997.

3. "A Study of Helium Liquefaction Cycles at Elevated Pressures," by Moses Minta, MS Thesis, MIT 1981.

4. Jones, R.E. and Smith Jr., J.L., "Design and Testing of Experimental Free-Piston Cryogenic Expander," in *Advances in Cryogenic Engineering* 45, Kluwer Academic/Plenum Publishers, New York, 2000.

5. Smith Jr., J.L., Brisson, J.G., Traum, M.J., Hannon, C.L., and Gerstmann, J., "Description of a High-Efficiency Floating Piston Expander for a Miniature Cryocooler", in *IMECE2002*, Vol. 3, Paper Number IMECE2002-33402.